

# THE SENSITIVITY OF CODA WAVE INTERFEROMETRY IN CONCRETE STRUCTURES IN DIFFERENT SCATTERING REGIMES

Patrik FRÖJD, Peter ULRIKSEN  
Department of Engineering Geology,  
Lund University, Sweden

John Ericssons Väg 1, SE-221 00, Sweden. Email: patrik.frojd@tg.lth.se

**Key words:** Coda waves, CWI, structural health monitoring, ultrasound, diffuse field

## Abstract

Coda wave interferometry (CWI) has been demonstrated to be a very sensitive tool for detecting early signs of damage in concrete. The choice of frequency in SHM applications, utilizing coda waves, is not straight-forward, as there is a trade-off in sensitivity and possible propagation distances. This study aims to provide some steps in establishing recommendations as to choice of frequency, when designing CWI SHM systems, based on expected size of damage and size of the monitored structure. To this end codas with widely different central frequencies were used to detect boreholes at different relative locations in the concrete. The results suggest that, for damage which can be simulated by drilled holes on the scale of a few mm, signals in the range of 50-150 kHz is suitable for SHM applications in large concrete structures.

## 1 INTRODUCTION

In concrete structures it is of great interest to be able to detect early signs of deterioration, as these quickly can lead to more serious damage. There exist a number of different non-destructive testing (NDT) methods which are suitable for implementation in structural health monitoring (SHM) systems, which can continuously monitor a structure for changes, many of which are based on propagating ultrasonic waves. However, traditional ultrasonic measurements can be problematic, in concrete, due to the severe scattering of the waves in the aggregates. This scattering redistributes energy from the coherent wave to a more diffuse propagation.

In coda wave interferometry (CWI), the trailing part of the transient signal is analyzed. These signals correspond to the diffuse field created by reflections from the boundaries and scattering from heterogeneities in the material. It has been shown that CWI is very sensitive to changes in the material, due to the fact that the trailing parts of the measured signal correspond to waves that have traversed a relatively large volume, and have thus traversed the damaged region repeatedly. These waves have been more affected by damage in the material than the parts corresponding to the direct propagation path. Analysis of coda waves is an attractive prospect for SHM applications, since not only the direct path between two transducers is probed, but a larger volume.

The literature describes numerous studies where CWI has been implemented in both NDT and SHM applications and investigated for its ability to detect early onsets of cracking in concrete [1]–[4]. There has been recent publications which report on methods to compensate for temperature effects on CWI measurements [5], [6] and to measure nonlinear effects in the monitored material [7], [8], thus furthering the usefulness of diffuse field measurements in SHM applications.

Interest in coda waves originated in seismic applications, and, though the frequencies of the waves in those applications are vastly different from those in NDT applications aimed at concrete structures, the basic principles remain the same.



The interaction between mechanical waves in concrete and the heterogeneities in the mix depends on the wavelength and the typical size of the heterogeneities. Following the naming convention used in the review by Planés and Larose [2], four frequency domains can be identified for scattering in concrete. The transition between regimes is smooth and depends greatly on the typical size of the aggregates used in the concrete mix.

The Stationary wave regime, for frequencies below 10-20 kHz, is mostly associated with modal analysis. In this regime the wavelength is on the same order of length as the structure as a whole, and thus much larger than the aggregates in the concrete. The interaction between the waves and the aggregates is mostly negligible. There is, however, reflections in boundaries of the structure, which will create a diffuse wave field, and thus give rise to a coda in a measured signal.

Larose et al. used signals in the 1 kHz range to track variations in a concrete building due to temperature variations [9] and Stähler et al. used signals in similar frequency ranges to monitor stress changes in the concrete during the launching of a bridge deck [10].

The simple scattering regime, for frequencies between the stationary wave regime and up to approximately 100-150 kHz, is the range commonly used for traditional ultrasonic investigation of concrete. Given a wave propagation speed of approximately 4300 m/s for compressional waves and 2500 m/s for shear waves, the wavelengths in this frequency domain is in the order of a couple of centimeters. This is commonly in the order of, and slightly larger than, the average size of the aggregates (and reinforcement bars) in concrete. The wave interact weakly with the heterogeneities and the codas in this regime thus consist of a mix of scatterings and reflections in boundaries.

There are several published accounts of coda wave analysis in concrete in this regime, where different changes to the structure successfully is detected. Works by Niederleithinger et al. [11], Stähler et al. [10], and Fröjd and Ulriksen [12] are examples where diffuse ultrasound, in the range of 50-70 kHz, is used to detect and track stress changes and/or cracking of concrete samples.

The multiple scattering regime, for frequencies between the simple scattering regime and up to approximately 1 MHz, is the range where the wavelengths of the ultrasound is typically shorter than the general size of the aggregates. In this regime the waves are strongly affected by the heterogeneity and the direct/coherent wave is strongly attenuated. Measured signals then mostly consists of a coda, created by multiple scatterings. Most publicized work on CWI in concrete operate in this regime, and it is here that the wave propagation can be said to behave like diffusion. The term “diffuse” is often used in literature as meaning either incoherent waves, which do not resist spatial averaging, or as intensity propagation which can accurately be described by the solution of the diffusion equation.

Examples of work in concrete CWI in the multiple scattering regime includes publications by Larose and Hall [13], Schurr et al. [3], and Zhang et al. [14]. Larose and Hall showed that they could detect variations of relative velocity in the concrete sample, due to stress changes, with a resolution of  $2 \cdot 10^{-5}$ , and other publications report on similarly high sensitivity.

The attenuation regime, for frequencies above 1 MHz, is the range where the ultrasound is so strongly attenuated, from both scattering and intrinsic absorption, that applications involving anything other than very small test objects in laboratories are infeasible. Applications with signals in this frequency regime thus have little use in practice, and is mostly neglected.

Locating damage in concrete, when using multiple scattered and reflected wave measurements, is not straight-forward due to the diffuse nature of the acquired signals. However, methods for locating damage has been proposed, based on modeling travel time variations and decorrelation of coda waves [15]–[17]. In these methods the multiply scattered, propagating wave fields are approximated as diffusion or radiative transfer, and an inversion process is implemented to fit these analytical models to experimentally measured data. This yields images presenting the location of a local change, with a resolution of approximately one scattering mean free path,  $l$ , which is defined as the average distance between two scattering events. Another important parameter is the transport mean free path,  $l^*$ , which is the average travel distance after which each wave packet contains no information as to its original direction. If isotropic scattering is assumed, then  $l = l^*$ . If the scatterings are anisotropic, then  $l < l^*$ , since more than one scattering event is required to completely randomize the direction. The imaging techniques will yield more accurate results if the anisotropy of the scattering process is considered, but this requires more information on the properties of the material [18].

The use of the radiative transfer approximation in the LOCADIFF algorithm, proposed by Planès et al., has been shown to give good results even if the location of damage is located in close proximity to the transducers, by also considering the direct propagating wave [19]. “Close proximity” in this regards means approximately one scattering mean free path. This means that the LOCADIFF method can be used to locate small changes also when using relatively low frequencies, in the simple scattering regime, as demonstrated by Niederleithinger et al. [11].

Clearly, there are numerous examples of useful applications of CWI in concrete in widely different frequency ranges. In practical SHM applications, with permanently installed transducers, it is often of interest to be able to monitor very large volumes, as civil structures can be many orders of magnitude larger than the test objects most often used in laboratory experiments. Depending on the circumstances, it might not be practical to operate in the multiply scattering regime, due to the severe attenuation of high frequency ultrasound in concrete. For traditional ultrasonic imaging (using only the coherent wave) it is easier to make recommendations as to the choice of frequency and transducer spacing, as resolution is often directly related to the wavelength and the range is given by the attenuation of the coherent wave. To the author’s knowledge, when using CWI, there exist no such recommendations. We therefore aim to investigate the usefulness of CWI in a wide range of frequencies, encompassing the three first scattering regimes. The usefulness is measured by the difference in sensitivity to changes and by the difference in transmission range.

In this paper the ability of CWI at different frequencies to detect the appearance of new scatterers in the concrete is compared. This is one step in being able to provide recommendations when implementing CWI in NDT or SHM applications of large concrete structures.

## 2 MATERIALS AND EQUIPMENT

The test object used in the study was an 800 x 211 x 8-cm concrete floor slab. Table 1 provides details on the concrete mix. The mix has a water-cement-ratio of 0.442 and the slab is reinforced with a steel mesh with a nominal diameter of 6 mm and 150 mm squares.

Due to the fact that signals with vastly different central frequencies were to be used, different transducer pairs were used. The stationary wave regime signal was transmitted between a pair of SM-6 3500Ω geophones from ION. The use of geophones as reciprocal transmitters and receivers of low frequency mechanical waves in concrete has previously been investigated by the authors [20]. The geophones have a major resonant frequency at 3.1 kHz. The simple- and multiple

scattering regime signals were all transmitted by Ferroperm Pz26 piezoceramic disks with diameter 37.7 mm and received by Ferroperm Pz37 piezoceramic disks with diameter 27 mm. Both types of piezo ceramic discs have a resonant frequency of about 500 kHz. All transducers yields vertical excitation.

The signals were generated by an Agilent 33500B waveform generator and amplified to 200 Vpp. All signals were sampled by an Agilent InfiniiVision DSO-X 3014A oscilloscope. Custom made switches enabled switching between the various transducer pairs.

Components	Values (kg/m <sup>3</sup> )
Sand	1006
Aggregate (8-11 mm)	704
Cement	406
Water	101
Superplasticizer (Sika HD 100)	3.8
Air entraining agent (SikaAer S)	0.4

Table 1: Composition of concrete.

### 3 EXPERIMENTAL PROGRAM

The excitation signals were all 5-cycle, Hanning-windowed, sinusoidal pulses with different central frequencies. Five different frequencies were used; 500, 250, 150, 50 and 3.1 kHz. In the concrete, these cover the three useful scattering regimes. A separate transducer pair was used for all transmission frequencies.

The point of the study was to investigate the influence of choice of frequency on the sensitivity of the CWI measurement to an extra scatterer, on the same order of magnitude as the aggregates in the concrete. The transducers were placed at a distance of approximately 20 wavelengths (based on the shear velocity). This corresponds to 10, 20, 33 and 100 cm for the 500, 250, 150 and 50 kHz signals respectively. The corresponding distance for the 3.1 kHz signal would be ~16 m, which is longer than the length of the slab. The geophone transducers were instead placed 4 m apart. For a structure of this size, regardless of where the transducers are placed, the measured signals will consist of waves which have been reflected in boundaries many times. The distance between the transducers is therefore not crucial. All signals had signal-to-noise ratios of >40 dB.

The five pairs of transducers were placed with these individual distances, all centered at the same location, roughly the center of the concrete slab. Figure 1 shows a sketch of the transducer placement. Each measurement was averaged 5 times, and was further put through a digital band-pass filter, centered on the central frequency of the signal.

The extra scatterers were introduced at different distances from the center line by drilling holes in the concrete. The holes were located 0, 5, 10, 20, 30 and 40 cm from the center line. Each hole was first drilled with a 4 mm diameter, then expanded to 8, 10 and 12 mm in steps. The holes were all ~1 cm deep. Eight measurements were made at each hole, at each hole diameter.

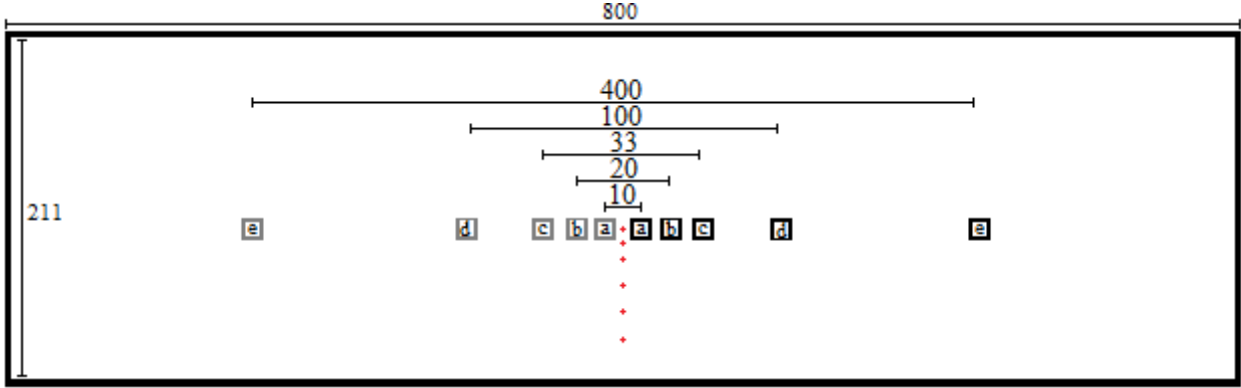


Figure 1: Layout of the concrete floor slab, transducers and bore holes. Dimensions given in cm. The transducer pairs denoted a-e in the figure were used for signals with frequencies 500, 250, 150, 50 and 3.1 kHz respectively. The transducers to the right of the center were used as transmitters and those to the left as receivers. The red crosses indicate the location of the boreholes. The boreholes are located 0, 5, 10, 20, 30 and 40 cm from the center line, between the transducers. The sketch is not to scale and the transducers were placed slightly off-center on the slab, due to other instrumentation on the concrete.

#### 4 DATA PROCESSING

In order to make estimations of the scattering properties of the concrete at the different frequency ranges, the diffusion equation was fitted to the measured signals. A solution of the diffusion equation, in a finite 3D cuboid structure with sides  $a$ ,  $b$  and  $c$ , assuming isotropic scattering and no ultrasonic flux out from the boundaries from the concrete, is given by [21]:

$$\begin{aligned} \langle E(x, y, z, t) \rangle = E_0 e^{-\sigma t} \{ & 1 + [g(x, x_0, a)g(y, y_0, b)g(z, z_0, c)] \\ & + [g(x, x_0, a) + g(y, y_0, b) + g(z, z_0, c)] \\ & + [g(x, x_0, a)g(y, y_0, b) + g(x, x_0, a)g(z, z_0, c) \\ & + g(y, y_0, b)g(z, z_0, c)] \} \end{aligned} \quad (1)$$

where

$$g(x, x_0, a) = \sum_{m=1}^{\infty} \cos\left(\frac{m\pi x}{a}\right) \cos\left(\frac{m\pi x_0}{a}\right) e^{-D\left(\frac{m\pi}{a}\right)^2 t} \quad (2)$$

Here  $\langle E(x, y, z, t) \rangle$  is the ensemble average energy density, and can be thought of as the time evolution of the slowly varying envelope of the coda energy. The model assumes an impulse excitation with amplitude  $E_0$  at point  $(x_0, y_0, z_0)$ , which is the source location.  $(x, y, z)$  is the receiver position and  $a$ ,  $b$  and  $c$  are the dimensions of the structure.  $D$  is the diffusivity, which describes the rate at which the diffusion covers an area. If the waves are strongly scattered in the material, the diffusion process is slower, which corresponds to a low value of  $D$ , and vice versa.  $\sigma$  is the dissipation rate, which describes the exponential decay of the coda.

By fitting the diffusion equation to the envelope of the measured signals, the scattering parameters  $D$  and  $\sigma$  can be estimated.

It should be noted that for the lower frequency signals, and in the stationary wave regime in particular, the “diffusivity” of the coda is created by boundary reflections rather than scattering, and the diffusion equation does not accurately describe the wave propagation. However, it could be of interest to get a rough approximation, though the values for the lowest frequency is rather specific for the geometry of the structure.

Using the estimated value of the diffusivity it is possible to estimate the transport mean free path by [22]:

$$l^* = \frac{dD}{v_e} \quad (3)$$

Where “d” is the dimensionality of the structure, which, in this case, is assumed to be 3 for the 500, 250 and 150 kHz signals and 2 for the 50 and 3.1 kHz signals. This is an approximation, based on the relationship between the wavelengths and the thickness of the slab; for the lower frequencies, the slab can be approximated as a 2D structure.  $v_e$  is the average velocity of the transport of energy, which could be thought of as the velocity of the envelope. A velocity of ~2500 m/s was measured in this setup, which agrees with the shear wave velocity in concrete.

The influence of the bore holes was evaluated by calculating the decorrelation of the coda in a time window  $[t_1, t_2]$ :

$$DC = 1 - \frac{\int_{t_1}^{t_2} \varphi^0(t) \cdot \varphi(t) dt}{\sqrt{\int_{t_1}^{t_2} \varphi^0(t)^2 dt \cdot \int_{t_1}^{t_2} \varphi(t)^2 dt}} \quad (4)$$

Where  $\varphi^0$  is the reference measurement waveform, before any hole is drilled, and  $\varphi$  is each subsequent measurement waveform. The time windows were chosen to include part of the waveforms with a high SNR. For the 500, 250, 150, 50 and 3.1 kHz signals were used the time windows [0.05, 0.5], [0.1, 1], [0.13, 1.1], [0.33, 4.0] and [20, 40] ms respectively. The lower frequency signals display longer coda trails due to their lower attenuation.

## 5 RESULTS AND DISCUSSION

Table 2 shows the diffusivity and dissipation parameters which provided the best fit of the diffusion equation to the measured waveforms. The yielded values are in general agreement with results from literature [23]. Also shown is the transport mean free path as estimated from the diffusivity. Examples of the different waveforms, as well as the diffusion approximation is shown in figure 2. The signals shown in figure 2 were collected with transducer distances 33 cm for the 500, 250 and 150 kHz signals, 1 m for the 50 kHz signal and 4 m for the 3.1 kHz signal.

Frequency (kHz)	Diffusivity (m <sup>2</sup> /s)	Dissipation (s <sup>-1</sup> )	Transport mean free path (cm)
500	8	13000	1.0
250	18	10000	2.1
150	39	7000	4.7
50	440	1200	35
3.1	~700	220	56

Table 2: Results from the fitting of diffusion equation of the measured waveforms.

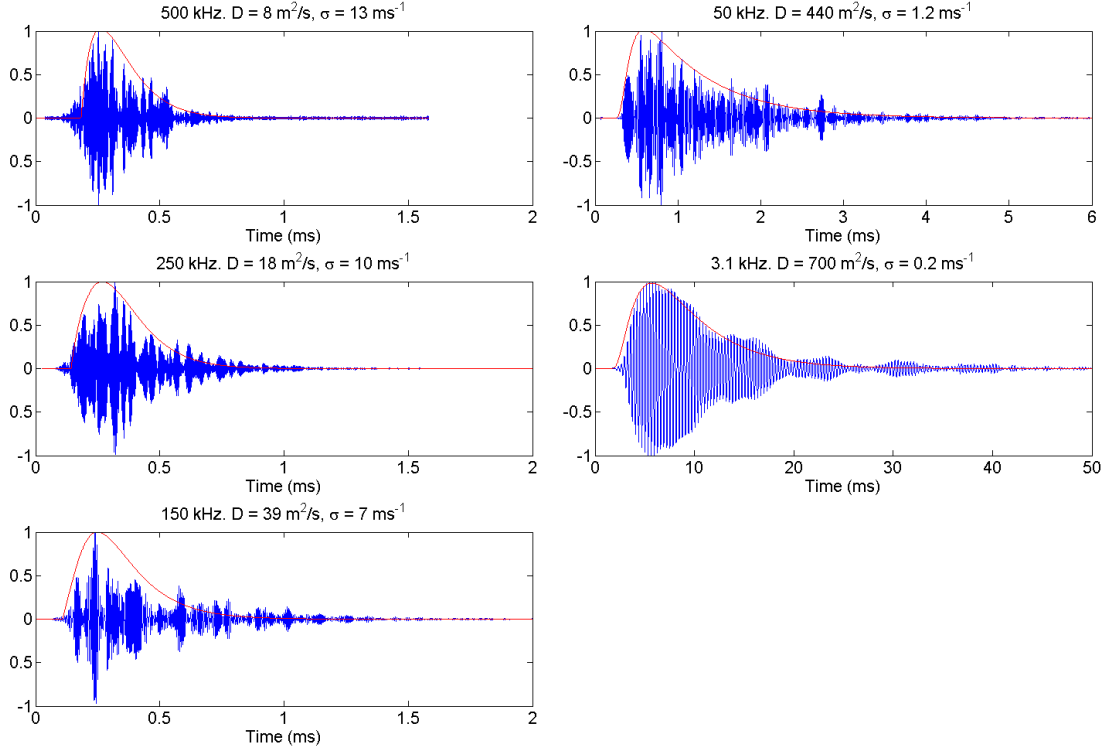


Figure 2: Measured waveforms for the different frequency signals. The diffusion approximation is shown in red, for each waveform.

Figure 3 shows the results from the coda decorrelation measurements for the different central frequencies and for the different boreholes. Each subplot shows measurements with one central frequency and each curve shows a specific distance between the borehole and the central line, according to figure 1. The y-axis shows coda decorrelation and the x-axis shows measurement number. Eight measurements were performed at each bore hole configuration, starting with eight measurements with no hole. The first of these measurements, with no hole, was used as reference signal in equation 4. The temperature was stable to within  $\pm 0.1$  °C.

From figure 3, it can be seen that the absolute level of decorrelation increases with frequency. This is intuitive, as a hole of a certain diameter will affect a signal with a small wavelength more than one with larger wavelength. However, the times at which the bore hole diameter was increased can clearly be seen even in the plots corresponding to the simple scattering regime (50 kHz) measurements. Even the smallest-diameter hole (4 mm) can be detected at this frequency. At this frequency, 4 mm corresponds to less than a tenth of a shear wavelength, and is smaller than the concrete aggregates and reinforcement bars. The ability to resolve an event depends on the stability of the baseline measurements (measurements 2-8 in this case), which, in turn, depends on signal-to-noise ratio and efficiency of implemented temperature compensation procedure. The standing wave regime signals (3.1 kHz) did show some indication of registering the larger-diameter drill holes, but not in any useful capacity. This is not surprising considering that the shear wavelength for these waves is  $\sim 80$  cm.

In the 500 kHz measurements, the last widening of the bore hole located directly between the transducers resulted in a decrease in absolute decorrelation. This is likely due to the signal being so distorted that the absolute value of the decorrelation is no longer relevant. A decorrelation of more than  $\sim 0.5$  could be said to indicate the signals simply being “very different”. There is thus a saturation of the decorrelation “damage indicator”.

The correlation between the distance of the hole to the direct line between the transducers and the decorrelation of the signals can clearly be seen in the figures. The sensitivity of the coda wave analysis decreases as the distance of the hole increase. This is caused by two factors: 1) the intrinsic absorption prevents far traveling waves from having influence on the measured signal. 2) The probability that a measured wave packet have passed a certain point decreases with distance to the transducers and the direct connecting line between them. The second phenomenon can be visualized as a sensitivity kernel, as described by e.g. Planés et al. [19] who showed that the width of the zone of high sensitivity between two transducers is approximately one transport mean free path. Clearly, the higher frequency signals (with shorter  $l^*$ ) display a more rapid decline in sensitivity as a function of distance. There does not seem to be a significant difference in the effect of the holes within this high sensitivity zone, which is in agreement with the statement that the resolution of sensitivity kernel-based imaging methods is in the order of  $l^*$ . The 150 kHz signal measurements seem to include the 10 cm-holes in this high sensitivity zone, which is more than the estimated  $l^*$ , but it should be noted that the estimation is a rough approximation. In general our measurements are in agreement with this theory.

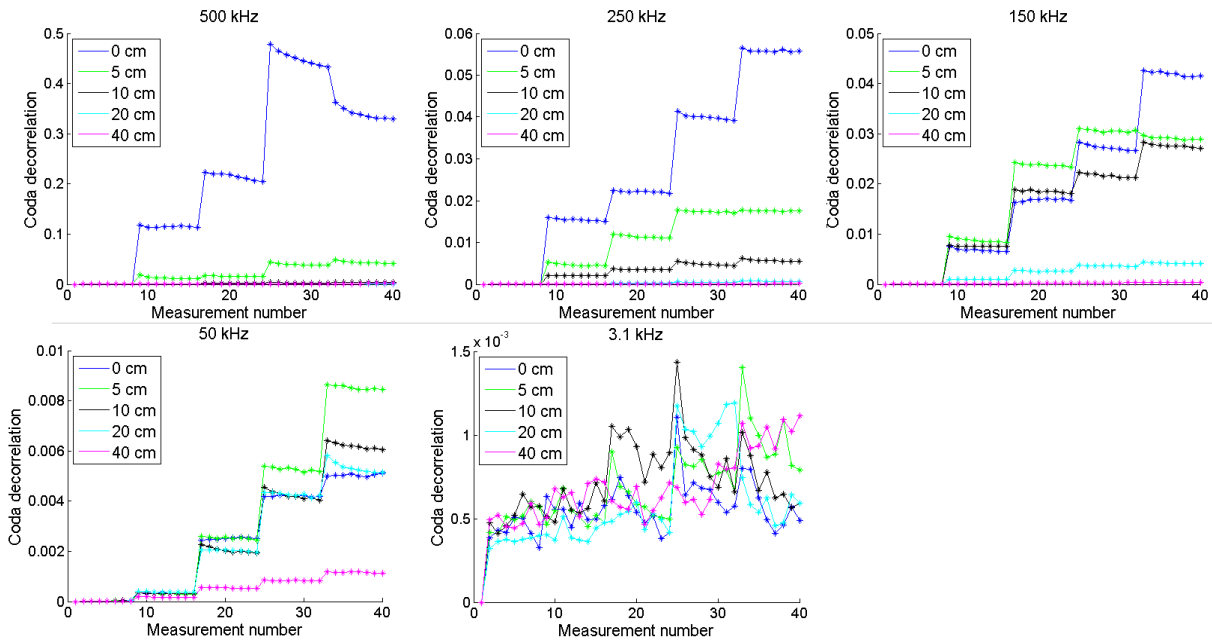


Figure 3: Decorrelation of the coda at different central frequencies. Boreholes are drilled at every eighth measurement, with diameters 4, 8, 10 and 12 mm. Each curve shows measurements with different distances between the holes and the center line between the transducer pair.

## 6 CONCLUSIONS

The ability to detect boreholes in concrete, smaller than the largest aggregates in the mix, using CWI in widely different scattering regimes has been investigated. As expected, it was found that the absolute decorrelation, and thus the sensitivity, was higher for the higher frequencies. However, it was shown that 50 kHz signals, in the simple scattering regime, can be used to detect holes, in the range of  $1/10 \lambda$  ( $\sim 4$  mm), in the concrete, with transmitting and receiving transducers placed at significantly larger distances than the higher frequency signals. Furthermore it was confirmed that the lower frequency signals could detect holes that were located further from the center line between the transducers. This is in agreement with the results presented by Planés et al.[19], which

suggests that the width of the sensitive area of diffuse waves, between two transducers, is approximately one transport mean free path.

It should also be noted that it is common to use chirp signals, over a wide range of frequencies. Such a signal was not included in this study, as we wanted to separate the influence of different frequency signals.

The results are some early steps to be able to provide recommendations to designers of SHM systems for concrete structures as to choice of frequency, and transducer placement, based on the size, and type, of expected damage and the general size of the structure to be monitored. For realistic concrete structures, which often are very large, the advantage in transmission range of simple scattering regime signals is great. And, clearly, 50-150 kHz signals can readily be used to detect mm scale damage, and higher frequency signals might not be necessary.

It has been shown that signals in the range of a few kHz, in the standing wave regime, is not able to detect cm-scale holes in concrete. However, previous studies have demonstrated the use of such signals for monitoring stress changes, and in such applications the very weak attenuation enables very long distances between transducers.

The authors realize that drilled holes are a very rough approximation of cracks in concrete. Further studies are thus planned, where similar comparisons are to be made for detecting more diffuse cracking and changes in stress in concrete.

## ACKNOWLEDGEMENTS

This work was supported by Swedish Research Council Formas [grant number 244-2012-1001].

## REFERENCES

- [1] Y. Lu and J. E. Michaels, "A methodology for structural health monitoring with diffuse ultrasonic waves in the presence of temperature variations.," *Ultrasonics*, vol. 43, no. 9, pp. 717–31, Oct. 2005.
- [2] T. Planès and E. Larose, "A review of ultrasonic Coda Wave Interferometry in concrete," *Cem. Concr. Res.*, vol. 53, pp. 248–255, 2013.
- [3] D. P. Schurr, J.-Y. Kim, K. G. Sabra, and L. J. Jacobs, "Damage detection in concrete using coda wave interferometry," *NDT E Int.*, vol. 44, no. 8, pp. 728–735, Dec. 2011.
- [4] O. Abraham, Y. Zhang, X. Chapeleau, O. Durand, and V. Tournat, "Monitoring of a Large Cracked Concrete Sample With Non-Linear Mixing of Ultrasonic Coda Waves," in *7th European Workshop on Structural Health Monitoring*, 2014, pp. 1412–1418.
- [5] Y. Zhang, O. Abraham, X. Chapeleau, L.-M. Cottineau, V. Tournat, A. Le Duff, B. Lascoup, and O. Durand, "Study of concrete's behavior under 4-point bending load using Coda Wave Interferometry (CWI) analysis," in *The 39th Annual Review of Progress in Quantative Nondestructive Evaluation*, 2013, no. September 2015, pp. 398–404.
- [6] Y. Zhang, O. Abraham, V. Tournat, A. Le Duff, B. Lascoup, A. Loukili, F. Grondin, and O. Durand, "Validation of a thermal bias control technique for Coda Wave Interferometry (CWI).," *Ultrasonics*, vol. 53, no. 3, pp. 658–64, Mar. 2013.
- [7] Y. Zhang, V. Tournat, O. Abraham, O. Durand, S. Letourneur, A. Le Duff, and B. Lascoup, "Nonlinear mixing of ultrasonic coda waves with lower frequency-swept pump waves for a global detection of defects in multiple scattering media," *J. Appl. Phys.*, vol. 113, no. 6, p. 064905, Feb. 2013.
- [8] B. Hilloulin, Y. Zhang, O. Abraham, A. Loukili, F. Grondin, O. Durand, and V. Tournat, "Small crack detection in cementitious materials using nonlinear coda wave modulation,"

- NDT E Int., vol. 68, no. September 2015, pp. 98–104, 2014.
- [9] E. Larose, J. de Rosny, L. Margerin, D. Anache, P. Gouedard, M. Campillo, and B. van Tiggelen, “Observation of multiple scattering of kHz vibrations in a concrete structure and application to monitoring weak changes,” *Phys. Rev. E. Stat. Nonlin. Soft Matter Phys.*, vol. 73, no. 1 Pt 2, p. 016609, Jan. 2006.
- [10] S. C. Stähler, C. Sens-Schönfelder, and E. Niederleithinger, “Monitoring stress changes in a concrete bridge with coda wave interferometry,” *J. Acoust. Soc. Am.*, vol. 129, no. 4, pp. 1945–1952, 2011.
- [11] E. Niederleithinger, “Coda wave interferometry used to localize compressional load effects in a concrete specimen,” *EWSHM-7th Eur. Work. Struct. Heal. Monit.*, pp. 1427–1433, 2014.
- [12] P. Fröjd and P. Ulriksen, “Amplitude and phase measurements of continuous diffuse fields for structural health monitoring of concrete structures,” *NDT E Int.*, vol. 77, pp. 35–41, Jan. 2016.
- [13] E. Larose and S. Hall, “Monitoring stress related velocity variation in concrete with a  $2.10^{-5}$  relative resolution using diffuse ultrasound,” *J. Acoust. Soc. Am.*, vol. 125, no. 4, pp. 1853–6, 2009.
- [14] Y. Zhang, O. Abraham, E. Larose, T. Planes, A. Le Duff, B. Lascoup, V. Tournat, R. El Guerjouma, L. M. Cottineau, and O. Durand, “Following stress level modification of real size concrete structures with CODA wave interferometry (CWI),” *AIP Conf. Proc.*, vol. 1335, no. 2011, pp. 1291–1298, 2011.
- [15] C. Pacheco and R. Snieder, “Time-lapse travel time change of multiply scattered acoustic waves,” *J. Acoust. Soc. Am.*, vol. 118, pp. 1300–1310, 2005.
- [16] E. Larose, T. Planes, V. Rossetto, and L. Margerin, “Locating a small change in a multiple scattering environment,” *Appl. Phys. Lett.*, vol. 96, no. 2010, pp. 2013–2016, 2010.
- [17] T. Planès, E. Larose, V. Rossetto, and L. Margerin, “LOCADIFF: Locating a weak change with diffuse ultrasound,” in *AIP Conference Proceedings*, 2013, vol. 1511, no. 1, pp. 405–411.
- [18] L. Margerin, T. Planès, J. Mayor, and M. Calvet, “Sensitivity kernels for coda-wave interferometry and scattering tomography: theory and numerical evaluation in two-dimensional anisotropically scattering media,” *Geophys. J. Int.*, vol. 204, pp. 650–666, 2016.
- [19] T. Planès, E. Larose, L. Margerin, and C. Sens-schönfelder, “Decorrelation and phase-shift of coda waves induced by local changes : multiple scattering approach and numerical validation,” *Waves in Random and Complex Media*, no. February 2015, pp. 1–10, 2014.
- [20] P. Fröjd and P. Ulriksen, “Efficiency of some voice coil transducers in low frequency reciprocal operations,” *J. Acoust. Soc. Am.*, vol. 137, no. 6, pp. EL490–5, Jun. 2015.
- [21] F. Deroo, J.-Y. Kim, J. Qu, K. Sabra, and L. J. Jacobs, “Detection of damage in concrete using diffuse ultrasound,” *J. Acoust. Soc. Am.*, vol. 127, no. L, pp. 3315–3318, 2010.
- [22] P. Sheng, *Introduction to Wave Scattering, Localization and Mesoscopic Phenomena*. San Diego: Academic Press Inc., 1995.
- [23] P. Anugonda, J. S. Wiehn, and J. A. Turner, “Diffusion of ultrasound in concrete,” *Ultrasonics*, vol. 39, no. 6, pp. 429–435, Oct. 2001.